Hindawi
Mathematical Problems in Engineering
Volume 2022, Article ID 3186744, 11 pages
https://doi.org/10.1155/2022/3186744

Research Article

Complexity Reduction for the Architecture Design of Large-Scale Public Buildings Based on Seismic Structure Simulation Technology

Xiji Hu,[1] Xingquan Li,[2] Mingwei Zuo,[3] and Wazid Michalak[4]

[1]*Assets and Logistics Section, Hebei Petroleum University of Technology, Chengde 067000, Hebei, China*
[2]*Department of Architectural Engineering, Hebei Petroleum University of Technology, Chengde 067000, Hebei, China*
[3]*Party and Government Office, Hebei Petroleum University of Technology, Chengde 067000, Hebei, China*
[4]*School of Computer Science, International Ataturk Alatoo University, Bishkek, Kyrgyzstan*

Correspondence should be addressed to Wazid Michalak; prof.michalak@mail.cu.edu.kg

Received 21 April 2022; Revised 23 May 2022; Accepted 30 May 2022; Published 14 June 2022

Academic Editor: Naeem Jan

In order to improve the seismic effect of large-scale public building architecture design, this paper studies the large-scale public building architecture design with the support of seismic structure simulation technology and improves the large-scale public building architecture design effect through simulation research. Furthermore, on the basis of the construction of the seismic performance evaluation system and the determination of the index weight, this paper assigns the index data to the sample table of the seismic performance checklist and establishes the seismic performance evaluation model based on the gray fixed-weight clustering method. Furthermore, using the seismic structure modeling technique described in this study, this paper assesses the seismic performance of public buildings. Finally, through experimental research, this paper verifies that the design method of large-scale public building architecture based on seismic structure simulation technology has certain practical effects.

1. Introduction

In terms of architectural functions, the top section uses an axis configuration of tiny bays, which necessitates the placement of extra walls. To organize the walls in the center, medium or small grids are necessary, while the bigger bays in the bottom section require fewer walls, although this will clash with the traditional structural design. The lower structure is subjected to large forces under the action of earthquakes, so the conventional design is to set up more wall columns in the lower part of the building to provide greater rigidity, and the upper part can gradually reduce the wall columns to reduce the stiffness. In order to meet the structural design of large bays in the lower part and small bays in the upper part of a comprehensive high-rise building, an effective method is to set up horizontal conversion components to realize the change of the axis network. However, this will bring some problems. The vertical stiffness of the structure near the transfer layer is prone to sudden changes, and the transfer layer will produce serious stress concentration. Once the force transmission path is missing, it will cause continuous collapse, which is very unfavorable for seismic design. At the same time, if the conversion member is located at the end of the building monomer, the large difference between the center of mass and the center of rigidity at the bottom of the structure will easily lead to torsion to form plane irregularities. Moreover, the end transformation causes the structure plane to be irregular, which is prone to torsional effects under the action of earthquakes. This requires that in the structural design, a reasonable vertical structure must be adopted, the upper and lower parts of the floor should have uniform and continuous rigidity, a reasonable transition should be made to avoid the occurrence of weak layers, and the position of the shear wall should be reasonably arranged on the plane to weaken the torsional effect.

With the passage of time, the construction industry's development tendency has experienced significant changes. While foreign countries such as Europe, the United States, and Japan no longer pursue architectural heights blindly, they instead use a variety of structural forms to achieve the ideal combination of architecture and art; while domestic architecture is constantly pursuing new heights, it is also moving toward diversified types, functions, high utilization rate, and other comprehensive development directions, such as Beijing's Jingcheng Building. It achieves the ideal balance of architectural purpose and artistic expression. Exquisitely designed high-rise buildings not only save land, increase the utilization rate, and bring more sufficient space for people to use, but also add landscape to the city and beautify people's living environment. From the perspective of urban construction and managers, with the continuous expansion of building space into the air, the density of people's settlement will increase accordingly, and people's daily life will also be transformed into three-dimensional space due to the close integration of horizontal and vertical traffic. These series of advantages make the development of high-rise buildings attract much attention. With the development of mechanics, the progress of structural analysis science, and the leap of information technology, the problems in practical engineering have been solved continuously, and the development of high-rise buildings will also enter a new stage. The constant refreshment of high-level officials in my country also announces that my country has begun to move toward the world and be in line with the world. China's population flow to cities has created dense urban areas, and high-rise and super high-rise buildings have filled the void. At present, my country's construction technology and structural design have reached the international advanced level and lead the trend of the world. The appearance of each city is constantly improved, and the development of each city is constantly advanced and renewed. People's way of life has been reshaped, and it is only natural for the senior executives to shoulder this important mission. High-rise buildings save the decreasing land area to a great extent and make more efficient use of building space.

In this paper, a large-scale public building architectural design research is carried out with the support of seismic structure simulation technology, and simulation research is used to improve the large-scale public building architectural design effect.

2. Related Work

The displacement-based design notion was introduced in [1] to enhance the bearing-capacity-based design approach, and performance-based seismic design was established as a result. The theoretical framework of performance-based design was presented by the California Institute of Engineers, and certain researchers in the United States, Japan, New Zealand, and other countries have done extensive study on it. Japan has obtained some research results in this aspect and implemented a new basic law of buildings based on performance-based design [2]. The FEMA 273 report recommends the use of the displacement influence coefficient method to evaluate the seismic performance and target displacement of the structure [3]. In addition to these methods, some foreign scholars have also proposed other performance-based seismic research methods. Although some of them are immature, they also provide new ideas for the development of performance-based seismic design. Reference [4] proposed an adaptive spectrum pushover analysis method, which reflects the dynamic characteristics of a structure with a high-order mode shape under non-fixed horizontal static loading. Reference [5] improved the capability spectrum method. Reference [6] proposed a function-based conceptual comprehensive design method. Reference [7] proposed a design method based on the yield displacement of the structure as the design index.

Reference [8] carried out a comparative analysis of the structural vertex displacement, interstory displacement, and bottom shear force and proposed an improved method for pushover's horizontal load mode and structural target displacement. Reference [9] proposed a research method for the deformation capacity of reinforced concrete frame columns and a performance-based seismic design. Reference [10] proposed a seismic plastic design research method based on energy balance, which can fully form the failure mechanism of strong columns and weak beams in building structures, improve the ductility of structures, and improve the ability of structures to resist earthquakes. Reference [11] proposed 5 seismic performance targets, 6 performance levels, and methods for implementing performance design for high-rise over-limit structures. Reference [12] put forward suggestions on the seismic design of over-limit high-rise buildings, including the performance level and seismic performance targets of performance design, displacement angle limits, and implementation methods. At present, the performance-based seismic design theory is not yet mature, and it is still a process of continuous improvement. We still need to conduct more in-depth research to make it more comprehensive and scientific in the future.

The most common method for predicting urban earthquake damage is "to select earthquake damage entities with characteristics to conduct detailed analysis and investigation, that is, select a certain number of structures based on structural characteristics and construction years, considering regional conditions and other conditions, and then analyze and study these buildings according to different types of earthquake damage." This approach is more thorough, but it is also more time consuming and requires a lot of expertise [13]. It is difficult to meet the requirements at this stage, so it brings great difficulty to the development of earthquake damage prediction work. Therefore, an earthquake disaster database is established for simple and fast earthquake damage prediction, and a unified earthquake damage prediction accuracy level is established. Once an earthquake occurs, its reliability can be tested through practice, and its deficiencies can be improved through data analysis.

With the increase of the number of floors, the structural complexity of the building is also increasing, and for such a

high-complexity large system, the structural vibration control is relatively difficult, mainly because of the large nonlinearity in the system and uncertainty [14]. Aiming at dealing with these complex large-scale system problems, scholars put forward a decentralized control strategy based on modern control theory. The so-called decentralized control is to divide a complex large system into several subsystems and use sub-controllers on each subsystem to implement control, and the control behavior of each subsystem will act simultaneously in each decentralized control system [15]. In [16], for large-scale structural systems, the structure is decomposed into several relatively small subsystems, and a decentralized control algorithm for the vibration response of high-rise frame structures under earthquake action is proposed. Reference [17] proposed a more convenient decentralized control algorithm, proved the stability and feasibility of the method theoretically, and simulated the structural vibration control problems of 8-story and 20-story frame structures under earthquake action. According to the decentralized control theory, the literature [18] decomposes a large system with complex structure into several subsystems and regards the interaction between the subsystems and the seismic disturbance as a generalized force acting on the subsystems. Then, the sliding mode control is adopted for each subsystem, and a decentralized stability control of substructure based on global stability is proposed. Reference [19] proposed a decentralized fuzzy iterative learning control algorithm, the principle of which is to combine the fuzzy logic theory and the iterative learning control algorithm principle, apply them to the vibration control of building structures, and use a decentralized control strategy. In the literature [20], the author studies the decentralized control of building structures under the action of earthquakes, gives corresponding improved control methods, and conducts simulation analysis of building structure models. Intelligent materials are becoming more important as building structure seismic performance criteria continue to increase. Researchers are increasingly focusing on their use in active control. Because smart materials have outstanding flexibility, intelligence, high efficiency, and great adaptability to the external environment, they are ideal for this application.

3. Simulation Technology of Seismic Structure

The comprehensive proportion of hazardous components of the overall structure (including foundation and basement) is determined according to the following formula:

$$R = \frac{\left(3.5n_{df} + 3.5\sum_{i=1}^{F+B+f} n_{dpci} + 2.7\sum_{i=1}^{F+B+f} n_{dsci} + 1.8\sum_{i=1}^{F+B+f} n_{dcci} + 2.7\sum_{i=1}^{F+B+f} n_{dwi} + 1.9\sum_{i=1}^{F+B+f} n_{drii} + 1.9\sum_{i=1}^{F+B+f} n_{dpmbi} + 1.4\sum_{i=1}^{F+B+f} n_{dsmbi} + \sum_{i=1}^{F+B+f} n_{dsbi} + \sum_{i=1}^{F+B+f} n_{dsi} + \sum_{i=1}^{F+B+f} n_{dsmi}\right)}{\left(3.5n_f + 3.5\sum_{i=1}^{F+B+f} n_{pci} + 2.7\sum_{i=1}^{F+B+f} n_{sci} + 1.8\sum_{i=1}^{F+B+f} n_{cci} + 2.7\sum_{i=1}^{F+B+f} n_{wi} + 1.9\sum_{i=1}^{F+B+f} n_{rti} + 1.9\sum_{i=1}^{F+B+f} n_{pmbi} + 1.4\sum_{i=1}^{F+B+f} n_{smbi} + \sum_{i=1}^{F+B+f} n_{sbi} + \sum_{i=1}^{F+B+f} n_{si} + \sum_{i=1}^{F+B+f} n_{smi}\right).} \quad (1)$$

In the formula, R is the comprehensive proportion of dangerous components of the overall structure; F is the number of upper structure layers; B is the number of basement structure layers; and f is the number of foundation layers.

$n_{df}, n_{dpci}, n_{dsci}, n_{dcci}, n_{dwi}$ are the numbers of dangerous foundations, central columns, side columns, corner columns, and wall components on the i-th floor.

$n_f, n_{pci}, n_{sci}, n_{cci}, n_{wi}$ are the total numbers of foundations, i-th floor central columns, side columns, corner columns, and wall components.

$n_{drii}, n_{dpmbi}, n_{dsmbi}$ are the numbers of the i-th floor trusses and middle beam and side beam members that are dangerous;

$n_{rii}, n_{pmbi}, n_{smbi}$ are the total numbers of the i-th layer roof trusses, middle beams, and side beams.

n_{dsbi}, n_{dsi} are the numbers of beams and roof panel members of the i-th level that are dangerous; n_{sbi}, n_{si} are the total numbers of beams and roof panel members at the i-th level.

n_{dsmi} is the number of the i-th layer envelope structural members that are dangerous.

n_{smi} is the total number of dangerous components of the i-th floor envelope.

It can be seen that the coefficients in the formula are 3.5 (foundation), 3.5 (center column), 2.7 (side column), 1.8 (corner column), 2.7 (wall), 1.9 (center beam), 1.4 (side beam), 1.0 (secondary beam), 1.0 (floor), 1.0 (enclosure), etc., reflecting the importance of different structural components of the house.

In the calculation points of the reinforced concrete frame structure, the strong and weak relationship of the components fully reflect the idea of "strong columns and weak beams" and "strong joints and weak rods."

3.1. Strong Columns and Weak Beams. The column end bending moment increase coefficient is used to reflect the design concept of "strong column and weak beam." It is stipulated that the design value of the bending moment at the column end should meet the requirements of (2) at the nodes of the first-level to fourth-level frames, except for the top layer and the joints of the frame columns and frame-supported beam columns whose axial compression ratio is less than 0.15:

$$\sum M_c = \eta_c \sum M_b. \quad (2)$$

In the formula, $\sum M_c$ is the sum of the design values of the bending moments of the clockwise or counterclockwise

cross section combination of the upper and lower column ends of the node.

$\sum M_b$ is the sum of the design values of the bending moments combined in the counterclockwise or clockwise direction of the left and right beam end sections of the node.

η_c is the increase factor of the bending moment at the column end of a frame. For the frame structure, the first, second, third, and fourth grades can be taken as 1.7, 1.5, 1.3, and 1.2, respectively.

3.2. Strong Section and Weak Rod. The failure of the frame joint will cause the pin-fixing failure of the beam end reinforcement in the joint, resulting in the frame becoming a hinged mechanism, and the consequences are more serious. In order to prevent the occurrence of this damage phenomenon, the shear force design value of the combination of the core area of the beam-column joints of the first-, second-, and third-level frames should be calculated according to the following formula:

$$V_j = \frac{\eta_{jb} \sum M_b}{h_{b0} - a_s'} \left(1 - \frac{h_{b0} - a_s'}{H_c - h_b}\right). \tag{3}$$

In the formula, V_j is the design value of the combined front force in the core area of the node.

h_{b0} is the effective height of the beam section, and the average value is used when the beam section heights on both sides of the node are not equal.

a_s' is the distance from the resultant point of the beam under compression to the compression edge.

H_c is the calculated height of the column, which can be the distance between the inversion points of the column at the upper and lower ends of the node.

h_b is the section height of the beam, and the average value is used when the beam section heights on both sides of the node are not equal.

η_{jb} is the strong joint coefficient. For the frame structure, 1.5 should be used for the first grade, 1.26 should be used for the second grade, and 1.2 should be used for the third grade.

The formula for calculating the design value of shear force for the combination of frame column and frame column is as follows:

$$V = \eta_{vc} \frac{\left(M_c^b + M_c^t\right)}{H_n}. \tag{4}$$

In the formula, H_n is the clear height of the column.

M_c^b, M_c^t are the design values of the combined bending moment of the upper and lower ends of the column in the counterclockwise or clockwise direction, respectively.

η_{vc} is the column shear increase factor. For the first, second, third, and fourth grades of the frame structure, they can be taken as 1.5, 1.3, 1.2, and 1.1, respectively. When substituting formula (2) into (4), we can get the following:

$$V = \eta_{vc} \eta_c \frac{\sum M_b}{H_n}. \tag{5}$$

Since the values of η_{jb} and η_{vc} tend to be consistent, η_c conservatively takes the maximum value of 1.7. Considering that the ratio of column height to beam height in the actual frame structure is about $1/4, a_s'$ is about 1/10 ~ 1/20 of h_b, and the middle value is 1/15, the ratio of the front force of the node to the design value of the column shear force is as follows:

$$\begin{aligned} \frac{V_j}{V} &= \frac{\eta_{jb} \sum M_b}{h_{b0} - a_s'} \left(1 - \frac{h_{b0} - a_s'}{H_c - h_b}\right) \eta_{vc} \eta_c \frac{\sum M_b}{H_n} \\ &= \frac{H_n}{\eta_c \left(h_{b0} - a_s'\right)} \left(1 - \frac{h_{b0} - a_s'}{H_c - h_b}\right) \\ &= \frac{4h_b}{1.3 \times \left(h_b - 2 \times 1/15 h_b\right)} \left(1 - \frac{h_b - 2 \times 1/15 h_b}{4h_b - h_b}\right) \\ &= 1.9306. \end{aligned} \tag{6}$$

We choose the fortification intensity of 7° to be consistent with subsequent models and since most cities in the nation have an earthquake-resistant fortification level of 7°. The frame structure's height is usually less than 24 metres, and the seismic grade is three. To summarize, the growth coefficient of the bending moment of the column end may be found to be 1.3. To some degree, the impact of the column and beam on the seismic resistance of the structure may be estimated to be about 1.3 : 1. From the calculation results of formula (6), it can be known that the influence of frame joints and frame columns on the seismic resistance of the structure is about 1.93 : 1.

For the weights of frame columns, frame beams, and nonstructural members, the foundation is taken as 3.5, the nonstructural members are taken as 1.0, and the frame column weight coefficient is taken as $(3.5 + 2.7 + 1.8)/3 = 2.7$. The frame beam weight coefficient is taken as $(1.9 + 1.4 + 1.0)/3 = 1.4$. The node connection weight is taken as $2.7 \times 1.9 = 5.22.7 \times 1.9 = 5.2$; the weight of the structural system is referred to as the "Seismic Code"; and the frame beam is used as the basis for adjustment, and it is taken as $1.4 \times 1.15 = 1.6$.

After sorting out the above weights, we can calculate the first-level indicator weights as follows:

$$\begin{aligned}
\text{base} &= \frac{3.5}{3.5+1.6+2.7+1.4+5.2+1.0} = 0.23,\\
\text{structural system} &= \frac{1.6}{3.5+1.6+2.7+1.4+5.2+1.0} = 0.10,\\
\text{frame column} &= \frac{2.7}{3.5+1.6+2.7+1.4+5.2+1.0} = 0.18,\\
\text{frame beam} &= \frac{1.4}{3.5+1.6+2.7+1.4+5.2+1.0} = 0.09,\\
\text{node connection} &\frac{5.2}{3.5+1.6+2.7+1.4+5.2+1.0} = 0.34,\\
\text{nonstructural components} &= \frac{1.0}{3.5+1.6+2.7+1.4+5.2+1.0} = 0.06.
\end{aligned} \tag{7}$$

The importance of components in the overall structure can be reflected by the degree of overall deformation of the structure caused by changes in the parameters of the components. The greater the influence on the deformation of the structural system is, the more important the component is, and the greater the corresponding weight coefficient is. In the structural system, due to the different degrees of contribution of each component to the overall seismic resistance of the structure, the reduction or increase of the resistance of each component in the same proportion will cause the structural deformation to increase or decrease in different degrees. The degree of seismic deformation is generally measured by the displacement angle between stories. The data sources used in this method and the results of nonlinear time-history analysis of structures under earthquake action are used in this paper. In the simulation, the parameters of a certain component are changed according to a certain proportion, so as to change the mean value of resistance, while keeping the resistance of other components unchanged. The change value of the displacement angle between layers of the structure is calculated as a measure of the importance of the components in the seismic performance of the structure.

The basic idea behind the time-history analysis method is to use the time function to introduce the dynamic action into the differential equation and then use the corresponding integral method to obtain the real dynamic response of the structure at each moment, as well as the response evolution process over time. There are two forms of time-history analysis: linear and nonlinear. The reaction of the structure under the action of general dynamic loads (such as frequent earthquakes) is the focus of linear dynamic analysis, and the response of the structure is in the linear elastic range. The nonlinear time-history analysis comprehensively considers the nonlinear properties of the structure such as the plastic development of the structure and the nonlinear connection element, which can meet the needs of the specific engineering for the analysis of the plastic development stage.

3.2.1. Establishment of Structural Dynamic Differential Equations. After a structural member begins to yield under the action of a rare earthquake, its restoring force is a function of the time function $\{y(t)\}$, and the nonlinear dynamic differential equation of the structure can be written as follows:

$$[M]\{\ddot{y}(t)\} + [C]\{\dot{y}(t)\} + \{F(y(t))\} = -[M]\{1\}\{\ddot{y}(t)\}. \tag{8}$$

According to (7), the nonlinear dynamic differential equation at time $t + \Delta t$ can be written as follows:

$$\begin{aligned}
&[M]\{\ddot{y}(t+\Delta t)\} + [C]\{\dot{y}(t+\Delta t)\} + \{F(y(t+\Delta t))\}\\
&= -[M]\{1\}\{\ddot{y}(t+\Delta t)\}.
\end{aligned} \tag{9}$$

By subtracting (8) and (9), the following formula can be obtained:

$$[M]\{\Delta\ddot{y}\} + [C]\{\Delta\dot{y}(t+\Delta t)\} + \{\Delta F\} = [M]\{1\}\{\Delta\ddot{y}\}. \tag{10}$$

When Δt is small, $\{\Delta F\}$ can be approximated by the tangent stiffness $[K(t)][K(t)]$, namely,

$$\{\Delta F\} = [K(t+\Delta t)] - \{\Delta y(t)\}. \tag{11}$$

Substituting formula (10) into (9), the following structural damped nonlinear dynamic incremental formula can be obtained:

$$[M]\{\Delta\ddot{y}\} + [C]\{\Delta\dot{y}\} + [K(t)]\{\Delta y\} = -[M]\{t\}\{\Delta\ddot{y}_g\}. \tag{12}$$

In the vibration formula (7), the damping matrix $[C]$ is represented by the viscous damping assumption theory, which can be obtained by converting the damping ratio of each mode shape of the measured system according to a certain method, which is called Rayleigh damping. Usually, it is represented by stiffness matrix $[K]$ and mass matrix $[M]$, as follows:

$$[C] = a[M] + b[K]. \tag{13}$$

The damping matrix must have the following properties to resolve the modal equations in a mode shape superposition analysis:

$$2w_n\xi_n = \{X_j\}^T [C]\{X_i\} = a\{X_j\}^T [M]\{X_i\} + b\{X_j\}^T [K]\{X_i\}, \tag{14}$$

$$\{X_j\}^T [C]\{X_i\} = 0\,(i \neq j). \tag{15}$$

Since the mass matrix and the stiffness matrix have orthogonal properties, formula (13) can be transformed into the following:

$$2w_n\xi_n = a + bw_n^2, \qquad \xi_n = \frac{1}{2w_n}a + \frac{w_n}{2}b. \tag{16}$$

It can also be expressed as follows:

$$\xi_n = \frac{1}{2w_n}a + \frac{w_n}{2}b. \tag{17}$$

It can be seen that the modal damping can be accurately obtained only at two frequencies, ω_i, ω_j, and the specific relationship is shown in the following formulas:

$$\xi_i = \frac{1}{2}\left(\frac{a}{\omega_i} + b\omega_i\right), \tag{18}$$

$$\xi_j = \frac{1}{2}\left(\frac{a}{\omega_j} + b\omega_j\right). \tag{19}$$

The following can be obtained from the above formula:

$$\left.\begin{aligned} a &= \frac{2\left(\xi_i\omega_j - \xi_j\omega_i\right)}{\omega_j^i - \omega_i^2}\omega_i\omega_j \\ b &= \frac{\left(\xi_j\omega_j - \xi_i\omega_i\right)}{\omega_j^i - \omega_i^2} \end{aligned}\right\}. \tag{20}$$

3.2.2. Solving the Structural Dynamic Equation. The time-history integration of the equilibrium equations at each point solves the structural dynamic equations. Modal and direct integration are the two basic ways of integration. In the modal integration, the overall response value of the structure must be derived by solving many modal integrals; hence, modal analysis is required. The essence of direct integration is to establish and solve equilibrium equations over a continuous time period.

(1) Newmark Method. The Newmark method has now become a more systematic method. The dynamic differential equation of the structure in the Newmark method is as follows:

$$M\ddot{u}_t + C\dot{u}_t + Ku_t = F_t. \tag{21}$$

u_t and $\dot{u}_t$ are expanded using Taylor series as follows:

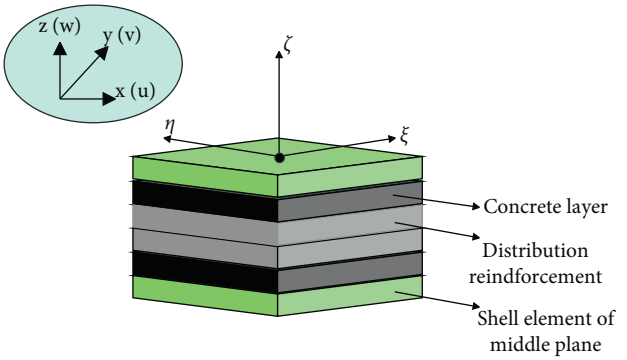

Figure 1: Layer shell element.

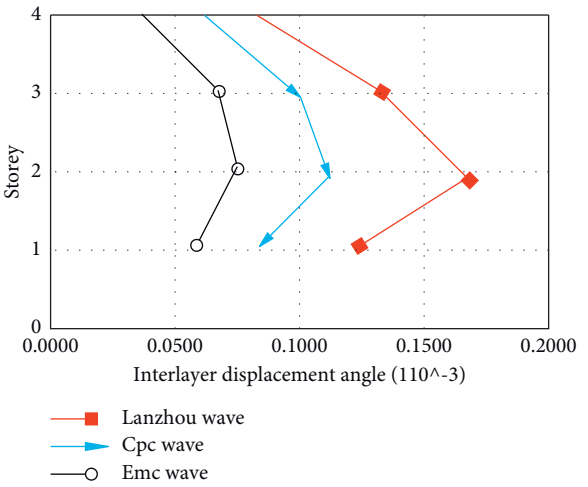

Figure 2: Interlayer displacement angle under three seismic waves.

$$u_t = u_{t-\Delta t} + \Delta t\dot{u}_{t-\Delta t} + \frac{\Delta t^2}{2}\ddot{u}_{t-\Delta t} + \frac{\Delta t^3}{6}\dddot{u}_{t-\Delta t} + \cdots, \tag{22}$$

$$\dot{u}_t = \dot{u}_{t-\Delta t} + \Delta t\ddot{u}_{t-\Delta t} + \frac{\Delta t^2}{2}\dddot{u}_{t-\Delta t} + \cdots. \tag{23}$$

When simplifying (21) and (22) by the Newmark method, we get the following:

$$u_t = u_{t-\Delta t} + \Delta t\dot{u}_{t-\Delta t} + \frac{\Delta t^2}{2}\ddot{u}_{t-\Delta t} + \beta\ddot{u}_{t-\Delta t}, \tag{24}$$

$$\dot{u}_t = \dot{u}_{t-\Delta t} + \Delta t\ddot{u}_{t-\Delta t} + \gamma\ddot{u}_{t-\Delta t}. \tag{25}$$

If the acceleration is assumed to be linear over the time step, we get the following:

$$\dddot{u}_t = \frac{\left(\ddot{u} - \ddot{u}_{t-\Delta l}\right)}{\Delta t}. \tag{26}$$

Substituting (25) into (23) and (24), we can obtain the standard form of the Newmark equation:

$$u_t = u_{t-\Delta t} + \Delta t\dot{u}_{t-\Delta t} + \left(\frac{1}{2} - \beta\right)\Delta t^2\ddot{u}_{t-\Delta t} + \beta\Delta t^2\ddot{u}_t, \qquad \dot{u}_t = \dot{u}_{t-\Delta t} + (1-\gamma)\Delta t\ddot{u}_{t-\Delta t} + \gamma\ddot{u}_t. \tag{27}$$

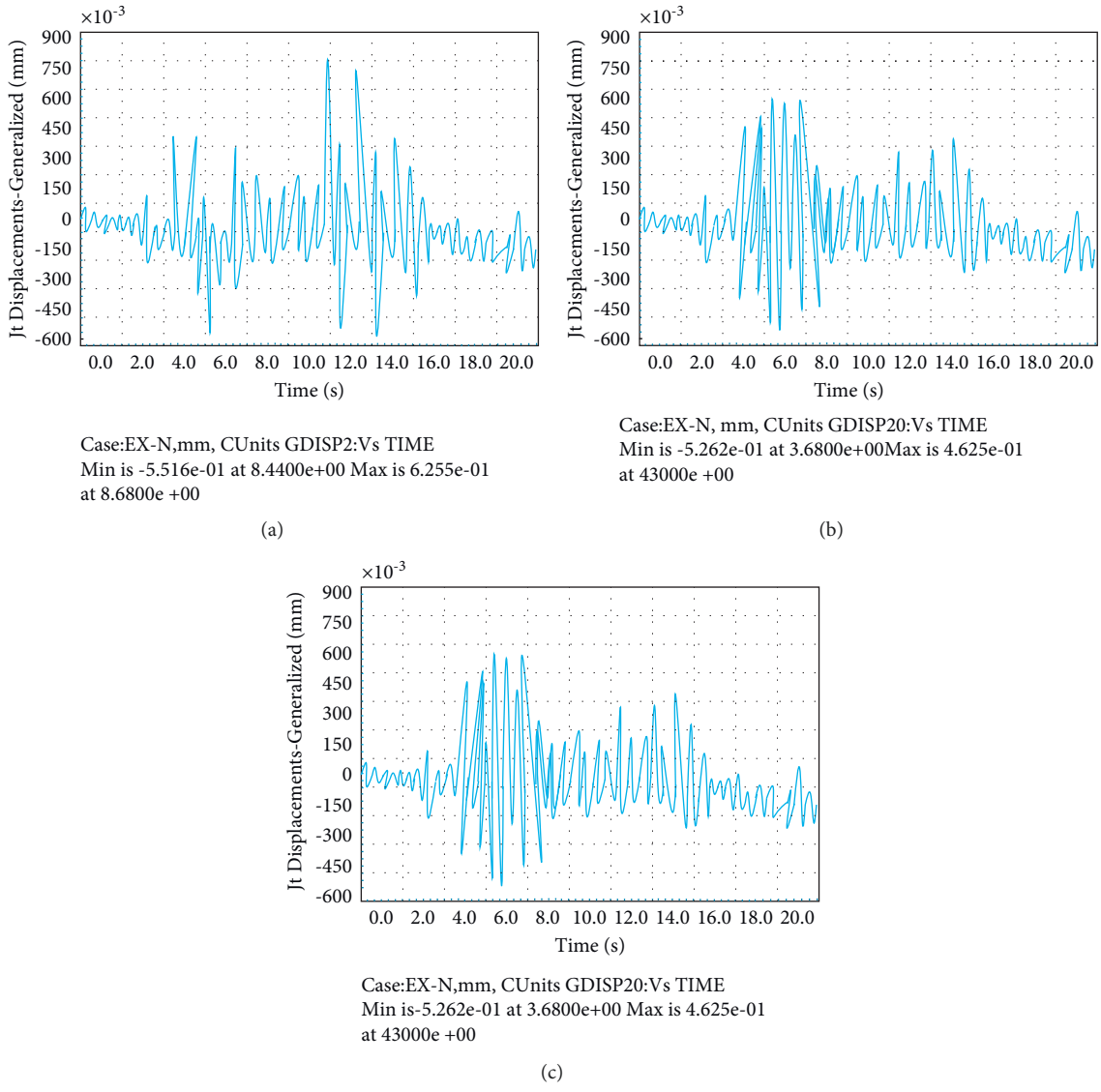

Figure 3: Time-history diagram of interlayer displacement on the second floor. (a) Emc seismic wave. (b) Cpc seismic wave. (c) Lanzhou seismic wave.

(2) HHT Method. The α coefficient is introduced to modify the conventional structural dynamic differential equation, and the Newmark method is used to solve the differential equation as follows:

$$M\ddot{u}_t + (1+\alpha)C\dot{u}_t + (1+\alpha)Ku_t = (1+\alpha)F_t - \alpha F_t + \alpha C\dot{u}_{t-\Delta t} + \alpha K u_{t-\Delta t}. \tag{28}$$

The HHT method takes a single parameter a, which can take values between 0 and −1/3.

For $a = 0$, this method is the same as the Newmark method for $\gamma = 0.5$ and $\beta = 0.25$ and is the same as the average acceleration method (also called the trapezoidal rule). When $\alpha = 0$, the obtained accuracy is the highest, but it will cause the vibration of the high-frequency mode shape. When α is a negative value, the high-frequency mode shape is attenuated quickly. In order to ensure the convergence of the results in the specific analysis, it is usually necessary to choose a negative value of α.

The effects of axial deformation, biaxial bending, torsional deformation, and biaxial shear deformation of components are primarily studied in this article, which uses frame elements to mimic reinforced concrete beams and columns. Thin-plate elements are used to depict floors and roofs in finite element software.

Nonlinear layered shell components are used in the autoclaved aerated fly ash concrete block. The layered shell element is based on composite materials' mechanical principles, and it may be split into several layers as required, with each layer having varied thicknesses and materials, as illustrated in Figure 1. This element takes into account the coupling effects between in-plane bending, in-plane shear, and out-of-plane bending.

In this paper, it is assumed that the bottom of the column is embedded on the top surface of the foundation, and the bottom of the column is restrained by a fixed end. The general steps for nonlinear time-history analysis are as follows:

(1) The calculation model of the structural member is established

(2) The seismic time-history curve defines and analyzes the working conditions

(3) Plastic hinges are defined and assigned to the frame

(4) The analysis required by the design is run

(5) The analysis results are viewed

The elastic-plastic time history analysis is carried out for the structure (model 0) with constant parameter settings. In this paper, the following three waveforms are analyzed and studied: Emc wave, Cpc wave, and LanZhou wave. Firstly, the above three kinds of seismic waves are input into the model in turn, and then the rare earthquake is multiplied by the corresponding scale coefficient, and finally the interlayer displacement is obtained. By changing the parameters involved in the index system, control a single variable to simulate in turn, and finally compare the analysis results with the original model analysis results.

(1) Analysis results of the original model

The natural period is $T_1 = 0.12895$, $T_2 = 0.12761$.

From Figure 2, we can see that the structural weak layer of the structure under the three seismic waves is in the second layer. The time-history curve of interlayer displacement in Figure 3 is consistent with the time-history curve of the seismic wave itself.

Color shades are used in cybernetics to convey the clarity of information, and the gray system is likewise called after color. "Black" denotes unknown information, "white" denotes information that is entirely certain, and "gray" denotes a situation in which some information is clear and other information is not. A "white system" is one with entirely clear information, a "black system" is one with unknown information, and a "gray system" is one with partly clear and partly ambiguous information.

Gray clustering is a technique of grouping observation indicators or observation objects belonging to the same class into a gray class based on the gray correlation matrix or the whitening weight function of gray numbers. Gray clustering based on the whitening weight function is primarily used to determine the degree to which observation indicators correspond to predetermined groups so that they may be treated differently. The specific process is as follows:

(1) Determine the whitening weight function and the gray class of the indicator.

In this paper, the seismic performance index is divided into 5 grades from low to high, and the gray class $h = 1, 2, 3, 4, 5$ is set. The evaluation index is defined to take a value between 0 and 10, and the seismic performance grade is set as $y_{k1}, y_{k2}, y_{k3}, y_{k4}, 0 < y_{k1} < y_{k2} < y_{k3} < y_{k4} < 10$.Then, each gray cluster gray class and its corresponding whitening weight function are as follows:

$$f_{k1}(c_{ij}) = \begin{cases} 1, & c_{ij} \in [0, y_{k1}] \\ \dfrac{10 - c_{ij}}{10 - y_{ij}}, & c_{ij} \in [y_{k1}, 10] \end{cases},$$

$$0 < y_{k1} < y_{k2} < y_{k3} < y_{k4} < 10,$$

$$f_{k,h+1}(c_{ij}) = \begin{cases} \dfrac{c_{ij}}{y_{kh}}, & c_{ij} \in [0, y_{kh}] \\ & c_{ij} \in [y_{kh}, y_{k,h+1}] \\ \dfrac{10 - c_{ij}}{10 - y_{k,h+1}}, & c_{ij} \in [y_{k,h+1}, 10] \end{cases}, \quad (29)$$

$$f_{k5}(c_{ij}) = \begin{cases} \dfrac{c_{ij}}{y_{k5}}, & c_{ij} \in [0, y_{k5}] \\ 1, & c_{ij} \in [y_{k5}, 10] \end{cases},$$

$$(h = 1, 2, 3).$$

(2) Calculate the gray evaluation weight matrix.

For the evaluation index C_{ij}, the gray rating coefficient of each gray category is processed by the weighted average principle, and the membership evaluation vector is obtained:

$$r_{ijh} = \frac{f_{kh}(c_{ij})^l \cdot h}{\sum_1^5 f_{kh}(c_{ij})^l \cdot h}. \quad (30)$$

The gray membership evaluation vector of evaluation index C_{ij} corresponding to each gray class is as follows:

$$R_{ijh} = [r_{ij1}, r_{ij2}, r_{ij3}, r_{ij4}, r_{ij5}]. \quad (31)$$

Then, the gray membership evaluation matrix of the secondary index C_{ij} corresponding to each gray class is obtained:

$$R_i = \begin{pmatrix} R_{i1} \\ R_{i2} \\ \vdots \\ R_{ij} \end{pmatrix} = \begin{pmatrix} r_{i11} & \cdots & r_{i15} \\ r_{i21} & \cdots & r_{i25} \\ \vdots & \ddots & \vdots \\ r_{ij1} & \cdots & r_{ij5} \end{pmatrix}. \quad (32)$$

(3) The algorithm determines the weight w_i, $(i = 1, 2, \ldots, n)$ of each index.

(4) The algorithm performs comprehensive evaluation.

Comprehensive evaluation can be achieved through the following 4 steps:

(1) The algorithm makes a comprehensive evaluation on the evaluation index C_{ij}, and the result is recorded as B_i, and there are

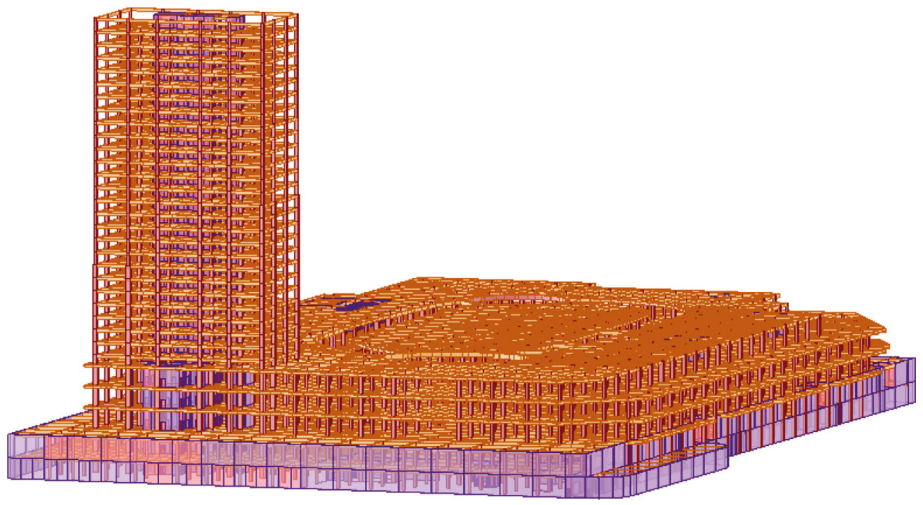

Figure 4: Schematic diagram of large-scale public building simulation.

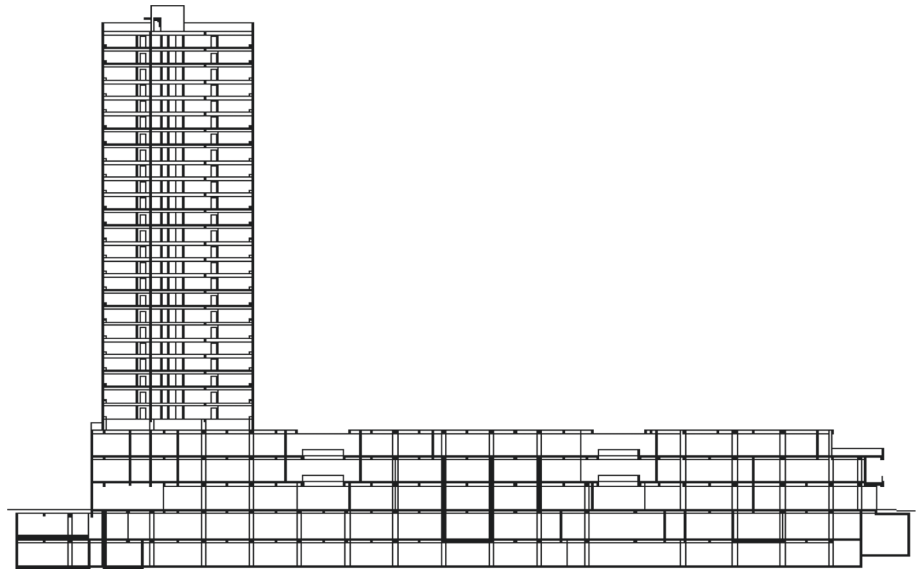

Figure 5: Sectional view of large-scale public building.

$$B_i = w_i \cdot R_i. \tag{33}$$

(2) From the comprehensive evaluation result B_i of C_{ij}, the subordinate degree evaluation matrix of the seismic performance index C_i for each evaluation gray class can be obtained as follows:

$$B = \begin{pmatrix} B_1 \\ B_2 \\ \vdots \\ B_k \end{pmatrix}. \tag{34}$$

(3) The algorithm makes a comprehensive evaluation of C_i, and the result is recorded as B; then, there are

$$B = w \cdot R = (b_1, b_2, \ldots, b_5). \tag{35}$$

(4) The five gray classes are assigned 1, 2, 3, 4, and 5 in turn, and $V = (1, 2, 3, 4, 5)$ is used to represent the equivalent vector of each evaluation gray class. Then, the evaluation value C of the seismic performance of the reinforced concrete frame structure house is as follows:

$$C = BV^T. \tag{36}$$

4. Architecture Design of Large-Scale Public Buildings Based on Seismic Structure Simulation Technology

Figure 4 shows the simulation research object of this paper. In this paper, the seismic performance simulation research of the building shown in Figure 4 is carried out through the seismic structure simulation technology.

Table 1: Structural natural vibration characteristics.

Vibration model	Cycle (s)	Translation coefficient ($X + Y$)	Torsion coefficient
1	2.9058	0.00 (0.00 + 0.00)	1.0000
2	2.8679	1.00 (1.00 + 0.00)	0.0000
3	2.4615	0.15 (0.00 + 0.15)	0.8585
4	1.9106	0.85 (0.00 + 0.85)	0.1515
5	0.8034	0.35 (0.30 + 0.05)	0.6565
6	0.7856	0.73 (0.70 + 0.04)	0.2727
7	0.5722	0.67 (0.22 + 0.46)	0.3333
8	0.5548	0.88 (0.09 + 0.79)	0.1212
9	0.4410	0.10 (0.04 + 0.06)	0.9090
10	0.4083	0.98 (0.65 + 0.33)	0.0202
11	0.3482	0.86 (0.56 + 0.30)	0.1414
12	0.3018	0.64 (0.40 + 0.23)	0.3636
13	0.2890	0.20 (0.06 + 0.13)	0.8080
14	0.2364	0.78 (0.09 + 0.69)	0.2222
15	0.2140	0.59 (0.56 + 0.03)	0.4141
16	0.2124	0.43 (0.37 + 0.05)	0.5757
17	0.1680	0.09 (0.05 + 0.05)	0.9191
18	0.1658	0.84 (0.06 + 0.78)	0.1616

The section view of the building is shown in Figure 5.

On the basis of the seismic structure simulation technology proposed in this paper, the seismic performance analysis of the above public buildings is carried out, and the output structural natural vibration characteristics are shown in Table 1.

Through the inspection and verification of Table 1, it can be seen that the effective quality coefficients of X and Y directions are all higher than 90%, which meets the requirements of the specification on effective quality coefficients. It is proved that the number of mode shapes selected for the structural model is also reasonable. Through the experimental research, it is verified that the design method of large-scale public building architecture based on seismic structure simulation technology has certain practical effects.

5. Conclusion

At present, comprehensive high-rise buildings have become an inevitable trend of social development. In the same building, it is necessary to divide the building into different parts along the height direction according to the change of function. Generally, the upper floors are used for residences, the middle floors are used for offices, and the lower floors are used for commercial purposes. The centralization of residential, catering, workplace, and other services preserves the country's land resources and considerably helps people's fast-paced life in contemporary society. The design of large-scale public buildings is carried out in this study with the use of seismic structure simulation technology, and the design impact of large-scale public buildings is enhanced by simulation research. Finally, through experimental research, this paper verifies that the design method of large-scale public building architecture based on seismic structure simulation technology has certain practical effects.

Data Availability

The data used to support the findings of this study are available from the corresponding author upon request.

Conflicts of Interest

The authors declare that they have no conflicts of interest.

References

[1] I. Othman, Y. Y. Al-Ashmori, Y. Rahmawati, Y. Mugahed Amran, and M. A. M. Al-Bared, "The level of building information modelling (BIM) implementation in Malaysia," *Ain Shams Engineering Journal*, vol. 12, no. 1, pp. 455–463, 2021.

[2] R.-R. Dong, "The application of BIM technology in building construction quality management and talent training," *Eurasia Journal of Mathematics, Science and Technology Education*, vol. 13, no. 7, pp. 4311–4317, 2017.

[3] X. Qin, Y. Shi, K. Lyu, and Y. Mo, "Using a TAM-TOE model to explore factors of Building Information Modelling (BIM) adoption in the construction industry," *Journal of Civil Engineering and Management*, vol. 26, no. 3, pp. 259–277, 2020.

[4] Y.-C. Kim, W.-H. Hong, J.-W. Park, and G.-W. Cha, "An estimation framework for building information modeling (BIM)-based demolition waste by type," *Waste Management & Research: The Journal for a Sustainable Circular Economy*, vol. 35, no. 12, pp. 1285–1295, 2017.

[5] M. N. Kocakaya, E. Namlı, and Ü. Işıkdağ, "Building information management (BIM), a new approach to project management," *Journal of sustainable construction materials and technologies*, vol. 4, no. 1, pp. 323–332, 2019.

[6] T. Mandičák, P. Mesároš, and M. Tkáč, "Impact of management decisions based on managerial competencies and skills developed trough BIM technology on performance of construction enterprises," *Pollack Periodica*, vol. 13, no. 3, pp. 131–140, 2018.

[7] L. Ustinovichius, V. Popov, J. Cepurnaite, T. Vilutienė, M. Samofalov, and C. Miedziałowski, "BIM-based process management model for building design and refurbishment," *Archives of Civil and Mechanical Engineering*, vol. 18, no. 4, pp. 1136–1149, 2018.

[8] T. Wei and Y. Chen, "Green building design based on BIM and value engineering," *Journal of Ambient Intelligence and Humanized Computing*, vol. 11, no. 9, pp. 3699–3706, 2020.

[9] S. M. Noor, S. R. Junaidi, and M. K. A. Ramly, "Adoption of building information modelling (bim): factors contribution and benefits," *Journal of Information System and Technology Management*, vol. 3, no. 10, pp. 47–63, 2018.

[10] E. Papadonikolaki, C. van Oel, and M. Kagioglou, "Organising and managing boundaries: a structurational view of collaboration with building information modelling (bim)," *International Journal of Project Management*, vol. 37, no. 3, pp. 378–394, 2019.

[11] Y. Y. Al-Ashmori, I. Othman, Y. Rahmawati et al., "BIM benefits and its influence on the BIM implementation in Malaysia," *Ain Shams Engineering Journal*, vol. 11, no. 4, pp. 1013–1019, 2020.

[12] C.-J. Chen, S.-y. Chen, S.-h. Li, and H.-t. Chiu, "Green BIM-based building energy performance analysis," *Computer-Aided Design and Applications*, vol. 14, no. 5, pp. 650–660, 2017.

[13] H. R. Abed, W. A. Hatem, and N. A. Jasim, "Adopting BIM technology in fall prevention plans," *Civil Engineering Journal*, vol. 5, no. 10, pp. 2270–2281, 2019.

[14] L. Joblot, T. Paviot, D. Deneux, and S. Lamouri, "Literature review of Building Information Modeling (BIM) intended for the purpose of renovation projects," *IFAC-PapersOnLine*, vol. 50, no. 1, Article ID 10518, 2017.

[15] P. Wu, R. Jin, Y. Xu, F. Lin, Y. Dong, and Z. Pan, "The analysis of barriers to bim implementation for industrialized building construction: a China study," *Journal of Civil Engineering and Management*, vol. 27, no. 1, pp. 1–13, 2021.

[16] I. Kim, J. Choi, E. A. L. Teo, and H. Sun, "Development of K-BIM e-Submission prototypical system for the openBIM-based building permit framework," *Journal of Civil Engineering and Management*, vol. 26, no. 8, pp. 744–756, 2020.

[17] A. Dainty, R. Leiringer, S. Fernie, and C. Harty, "BIM and the small construction firm: a critical perspective," *Building Research & Information*, vol. 45, no. 6, pp. 696–709, 2017.

[18] A. Ahankoob, K. Manley, C. Hon, and R. Drogemuller, "The impact of building information modelling (BIM) maturity and experience on contractor absorptive capacity," *Architectural Engineering and Design Management*, vol. 14, no. 5, pp. 363–380, 2018.

[19] M. Deng, C. C. Menassa, and V. R. Kamat, "From BIM to digital twins: a systematic review of the evolution of intelligent building representations in the AEC-FM industry," *Journal of Information Technology in Construction*, vol. 26, no. 5, pp. 58–83, 2021.

[20] S. Ahmed, "Barriers to implementation of building information modeling (BIM) to the construction industry: a review," *Journal of civil engineering and construction*, vol. 7, no. 2, p. 107, 2018.